The Effect of Temperature and Active layer thickness on the Performance of $CH_3NH_3PbI_3$ Perovskite Solar Cell: A Numerical Simulation approach

Hassan Abdulsalam[*1], Garba Babaji[2] and Habu Tela Abba[1]

[1]Department of Physics, Yobe State University, Damaturu P.M.B. 1144, Yobe Nigeria
[2]Department of Physics, Bayero University, Kano P.M.B. 3011, Kano Nigeria
[*]*Corresponding author Email*: hassanklinsmann@gmail.com

Abstract: In this work, General-purpose Photovoltaic Device Model (GPVDM) software was used to investigate the performance of a perovskite solar cell with $CH_3NH_3PbI_3$ as its active layer. GPVDM is a free general-purpose tool for simulation of light harvesting devices. The model solves both electrons and holes drift-diffusion, and carrier continuity equations in position space to describe the movement of charge within the device. The model also solves Poisson's equation to calculate the internal electrostatic potential. Recombination and carrier trapping are described within the model using a Shockley-Read-Hall (SRH) formalism, the distribution of trap states can be arbitrarily defined. The software gives an output that contains the Current-Voltage (I-V) characteristic curves**.** A study into the effect of active layer thickness and temperature on the performance of the solar cell device was carried out. The optimal active layer thickness was found to be 3×10^{-7}m. When the thickness exceeds 3×10^{-7} m, then the efficiency drops. At the optimal thickness of 3×10^{-7}m, the devices were found to have power conversion efficiency up to 14.7%. On other hand the fill factor (FF) decreases as the thickness increases. The FF is highest at active layer thickness of 1×10^{-7}m. The effect of device temperature also studied and the optimal working temperature was found to be 300 K, where power conversion efficiency and FF are 15.4 % and 0.76 respectively.

1. Introduction

Methyl ammonium lead iodide, $CH_3NH_3PbI_3$ is a semiconducting material with a direct bandgap of 1.66 eV [1] and 1.55 eV [2]. It has both interesting optical and electronic properties that have been actively investigated during the past two decades. Its ability to absorb light over the whole visible solar emission spectrum makes it a good light-harvesting active layer for organic-

inorganic hybrid solar cells solar cells. Solar cell efficiencies of devices using $CH_3NH_3PbI_3$ and its likes have increased from 3.8% in 2009 [3] to a certified 20.1% in 2014, making this the fastest-advancing solar technology [4]. According to detailed balance analysis, the efficiency limit of perovskite solar cells is about 31%, which approaches the Shockley-Queisser of gallium arsenide which is 33% [5].Their high efficiencies and low production costs make perovskite solar cells a commercially attractive option.

The overall photovoltaic properties of solar cells are strongly dependent on the fabrication process, holes and electrons transport layers, nanoporous layers, interfacial microstructures, and crystal structures of the perovskite compounds [6]. At about 330 K $CH_3NH_3PbI_3$ exist in cubic crystal system, as the temperature decreases to about 236 K, the cubic phase is transformed into the tetragonal phase. As the temperature decreases lower to about 177 K, the tetragonal phase is transformed into orthorhombic crystal systems [7]. From above it is evident that temperature affects the crystal structures of $CH_3NH_3PbI_3$, and in turn the crystal structures of the perovskite-type compounds, strongly affect the electronic structures such as energy band gaps and carrier transport. The method of fabrication of methyl ammonium lead iodide film determines its thickness and the thickness in turn affect its optical properties and structures.

It was experimentally found that once the film thickness significantly exceeded the carrier diffusion lengths in $CH_3NH_3PbI_3$, the efficiency declined sharply [8]. In this work, effect of temperature and thickness of light harvesting active layer $CH_3NH_3PbI_3$ in particular on the overall performance of $CH_3NH_3PbI_3$ perovskite solar cell was determined numerically using General-purpose Photovoltaic Device Model (GPVDM).

2. Theoretical Background

The main electrical parameters of a solar can be analyzed by studying its current-voltage characteristics curve. Some of these parameters are: short circuit current (I_{sc}), open- circuit voltage(V_{oc}), maximum power point voltage (V_{mpp}), maximum power point current (I_{mpp}), maximum power point (MPP), fill factor (FF) and power conversion efficiency (η). The short circuit current, I_{sc} is current when voltage is equals to zero, and open circuit voltage, V_{oc} is voltage when current equals to zero. Maximum power point voltage (V_{mpp}) and Maximum Power Point Current (I_{mpp}) are the voltage and current respectively when the power output is the greatest. The maximum power point MPP is the point at which the product of the current and voltage equal the greatest value. The fill factor FF is the ratio of the maximum power point by a solar cell and the product of V_{oc} and J_{sc}. Empirically the FF is given by [9]:

$$FF = \frac{v_{oc} - ln(v_{oc} + 0.72)}{v_{oc} + 1} \qquad (1)$$

Where v_{oc} is normalized V_{oc} and it is given by

$$v_{oc} = \frac{q}{nkT} V_{oc} \qquad (2)$$

The conversion efficiency is calculated as the ratio between the maximal generated power and the incident power. Solar cells are measured under the Standard Test Conditions (STC), where the incident light is described by the AM1.5 spectrum and has an irradiance of 1000 W/m^2 [10].

3. Methodology

3.1 General-purpose Photovoltaic Device Model (GPVDM)

General-purpose Photovoltaic Device Model (GPVDM). GPVDM is a free general-purpose tool for simulation of light harvesting devices. The model solves both electrons and holes drift-diffusion, and carrier continuity equations in position space to describe the movement of charge within the device. The model also solves Poisson's equation to calculate the internal electrostatic potential. Recombination and carrier trapping are described within the model using Shockley-Read-Hall (SRH) formalism, the distribution of trap sates can be arbitrarily defined. A more detail description of the model can be found in the software manual [11].The software gives an output that contains the Current-Voltage (I-V) characteristic curves [12].
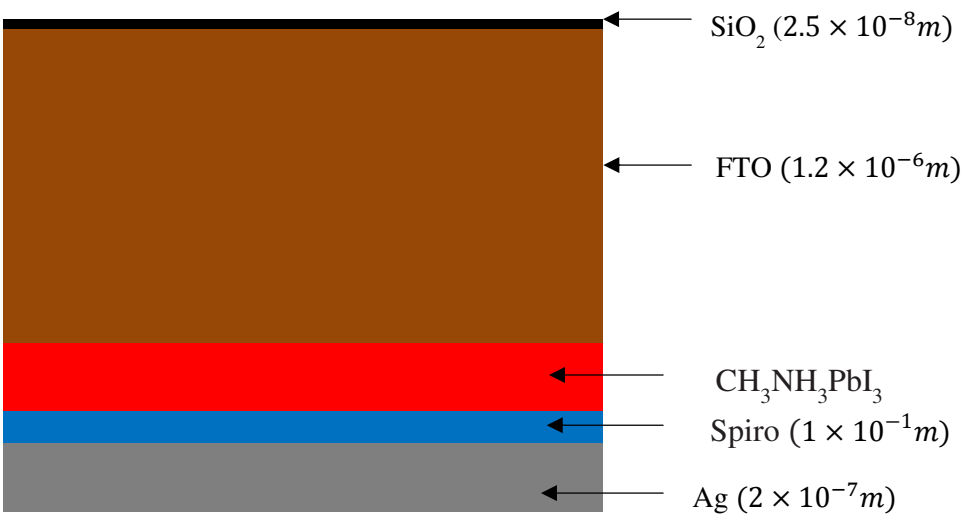
3.2 Device Structure

SiO_2 $(2.5 \times 10^{-8} m)$

FTO $(1.2 \times 10^{-6} m)$

$CH_3NH_3PbI_3$

Spiro $(1 \times 10^{-1} m)$

Ag $(2 \times 10^{-7} m)$

Fig: 1. Schematic representation perovskite solar cell, their thickness is given in bracket [11].

3.3 Simulation Parameters

The $CH_3NH_3PbI_3$ (Light harvester active layer) parameters used for the simulation are taken from GPVDM built-in default parameters, these are shown in the Table 1.

Table 1 Parameters used for the simulation

Parameters	Value
Electron trap density	8.6661×10^{24} m^{-3} eV^{-1}
Hole trap density	1.79044×10^{24} m^{-3} eV^{-1}
Electron tail slope	0.04 eV
Hole tail slope	0.04 eV
Electron mobility	0.0001 m^2 V^{-1} s^{-1}
Hole mobility	0.0001 m^2 V^{-1} s^{-1}
Relative permittivity	3
Number of traps	5 bands
Free electron to Trapped electron	3.22404×10^{-21} m^{-2}
Trapped electron to Free hole	6.43422×10^{-19} m^{-2}
Trapped hole to Free electron	2.66764×10^{-21} m^{-2}
Free hole to Trapped hole	6.38107×10^{-20} m^{-2}
Effective density of free electron states	5×10^{26} m^{-3}
Effective density of free hole states	5×10^{26} m^{-3}
Bandgap	1.6 eV

3.4 The Simulation

In this work, the simulation was run twice; the first for different set $CH_3NH_3PbI_3$ layer thickness and the second for different set of temperature. During the first simulation process, the thickness of perovskite ($CH_3NH_3PbI_3$) layer was optimized varying it from 1 x 10^{-7}m to 6 x 10^{-7} in a step of 1 x 10^{-7}m, i.e. the thickness that gives the highest efficiency. The optimal thickness obtained in the first simulation was used in the second simulation. Here the temperature was varied from 300K to 350K in a step of 10 K.

4. Results

Current-Voltage (I-V) characteristic curves obtained in the first and second simulations are shown in Figures 2and 3 respectively. The short circuit current (I_{sc}), open-circuit voltage (V_{oc}), maximum power point voltage (V_{mpp}), and maximum power point current (I_{mpp}) were deduced from the Current-Voltage (I-V) characteristic Curves in both simulations, and these are tabulated in Tables 2 and 3 along with fill factor, the maximum power point (mpp) and efficiency.
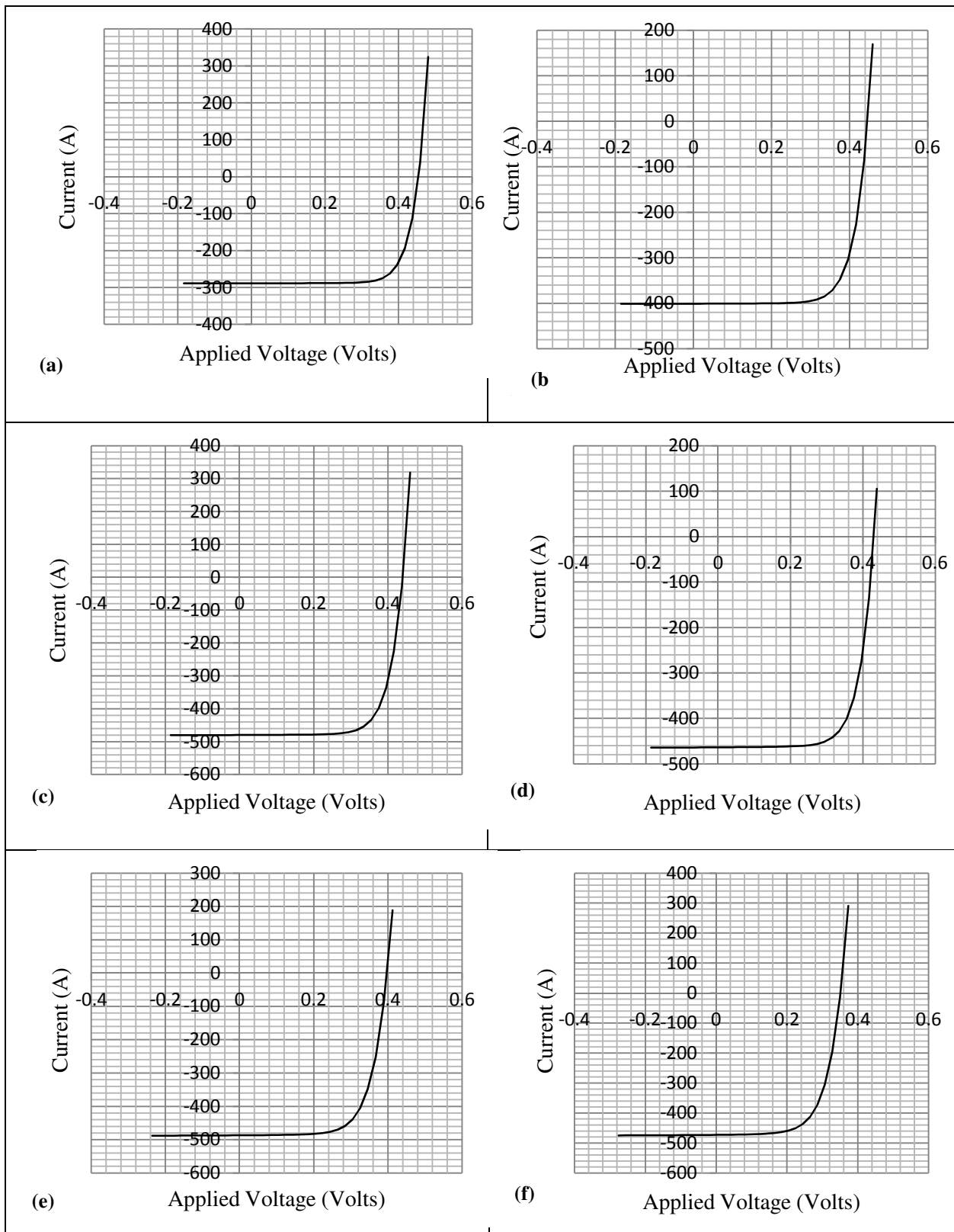
Fig. 2. Current-vintage (I-V) curve with active layer thickness: (a) $1 \times 10^{-7} m$
(b) $2 \times 10^{-7} m$ (c) $3 \times 10^{-7} m$ (d) $4 \times 10^{-7} m$ (e) $5 \times 10^{-7} m$ (f) $6 \times 10^{-7} m$

Table. 2. Solar cell parameters for different active layer thickness

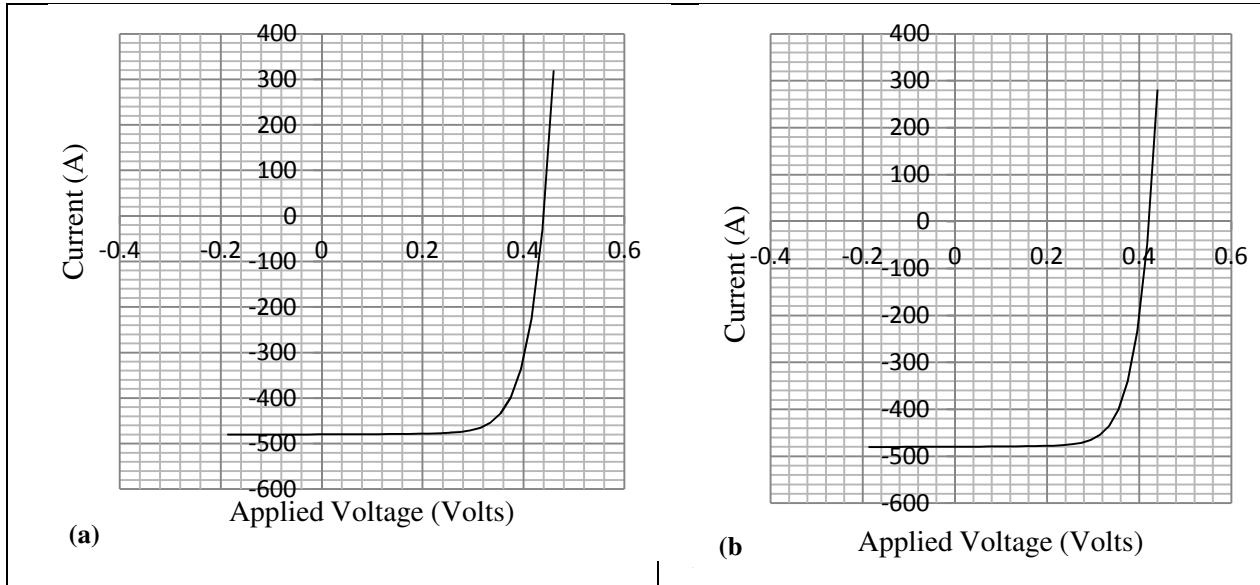| Thickness	Voc	Isc	Vmpp	Impp	FF	MPP	Conversion Efficiency %
1.00E-07	0.450	289	0.39	250	0.75	97.50	9.8
2.00E-07	0.450	401	0.37	360	0.74	133.20	13.3
3.00E-07	0.420	480	0.32	460	0.73	147.20	14.7
4.00E-07	0.430	464	0.36	400	0.72	144.00	14.4
5.00E-07	0.395	488	0.31	440	0.71	136.40	13.6
6.00E-07	0.350	470	0.26	420	0.66	109.20	10.9

(a) **(b**

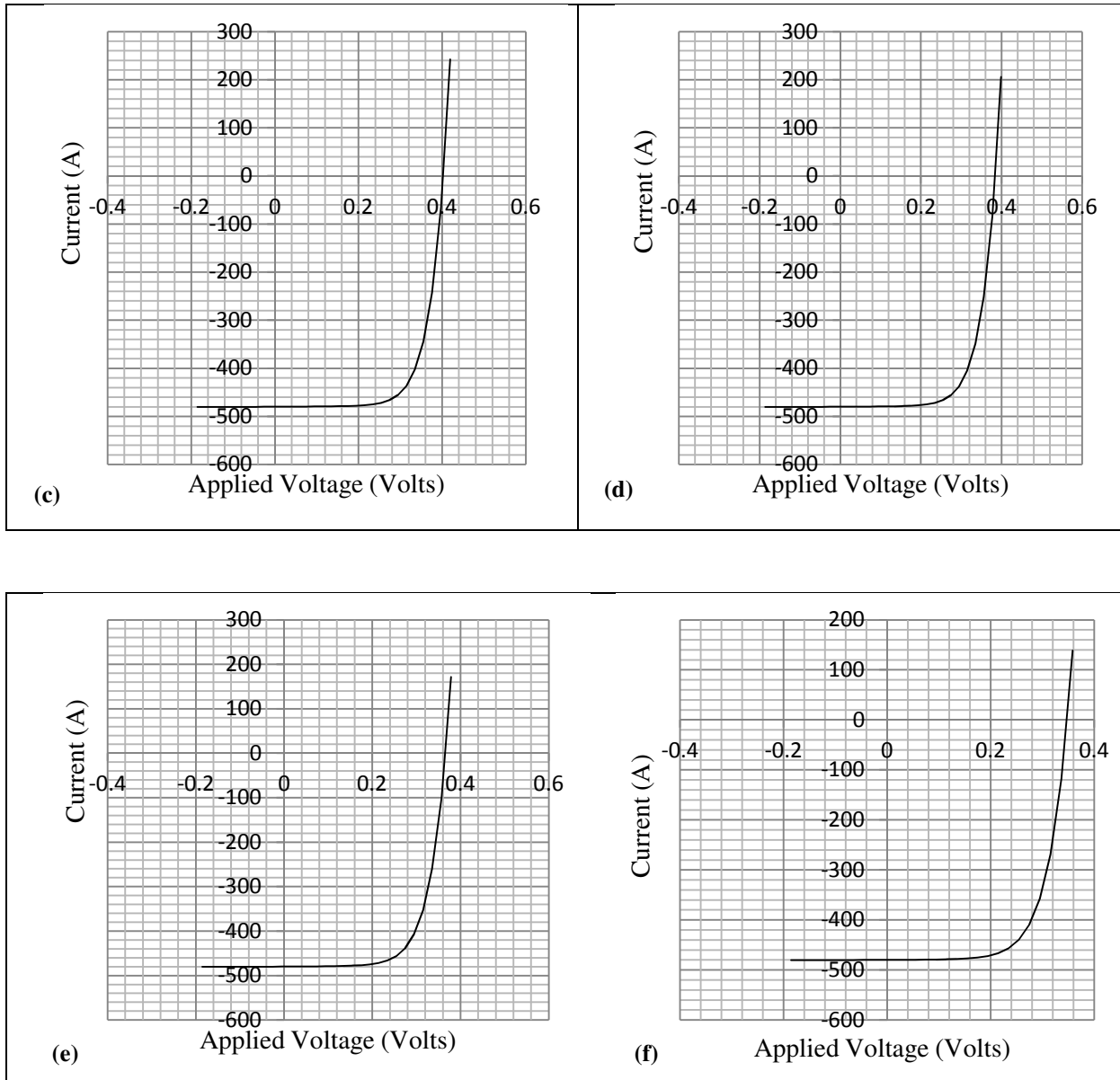**Fig. 3 (a, b).** Current-vintage (I-V) curve for Device temperature: (a) 300 K (b) 310 K

Fig. 3 (c, d, e, f). Current-vintage (I-V) curve for Device temperature: (c) 320 K (d) 330 K
(e) 340 K (f) 350 K

Table 3 Solar cell parameters for different device temperature

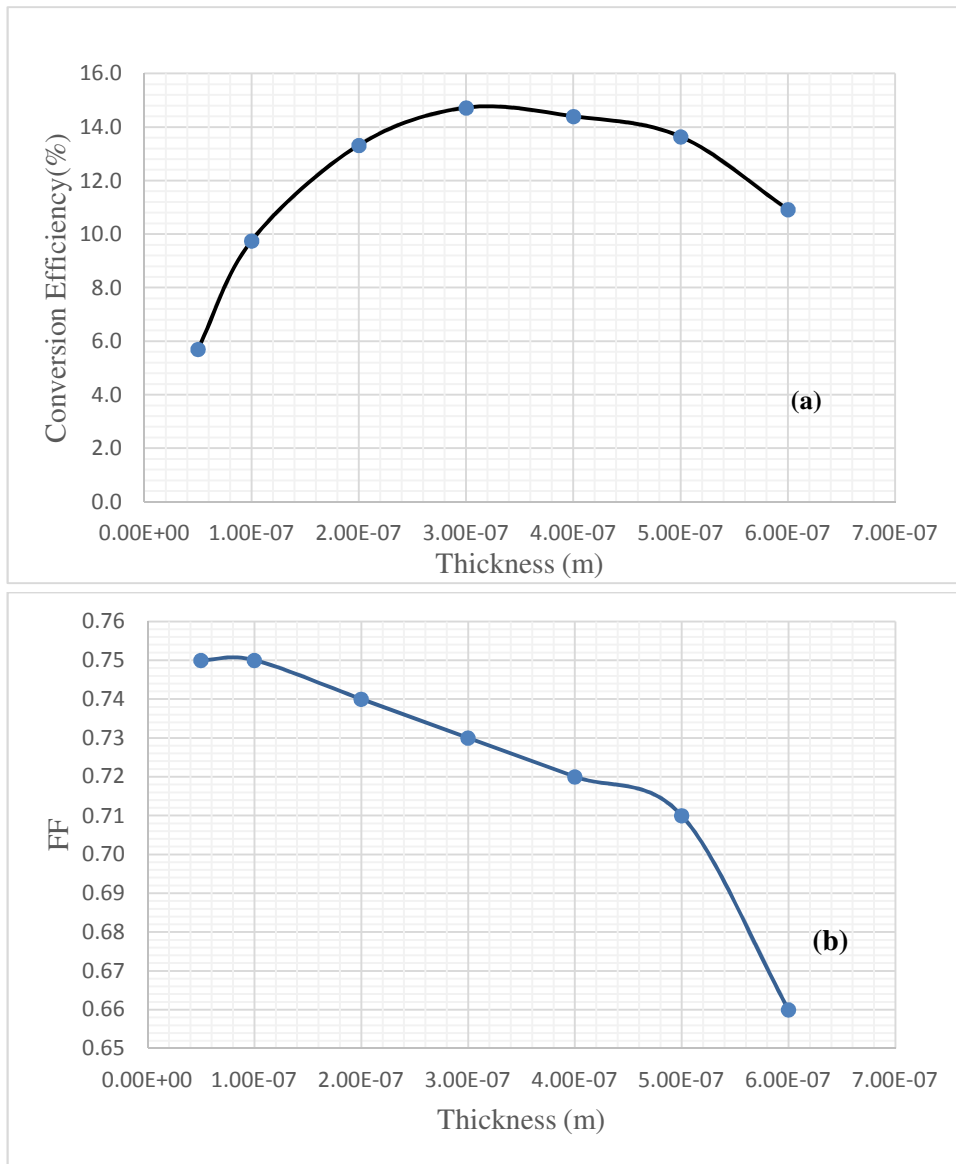| Temperature (^{0}K)	Voc	Isc	Vmpp	Impp	FF	MPP	Conversion Efficiency %
300	0.420	480	0.35	440	0.76	154.00	15.4
310	0.420	480	0.33	440	0.72	145.20	14.5
320	0.405	480	0.31	440	0.70	136.40	13.6
330	0.385	480	0.305	420	0.69	128.10	12.8
340	0.365	480	0.29	400	0.66	116.00	11.6
350	0.350	480	0.25	420	0.63	105.00	10.5

Fig. 4. Graph representing the variation of **(a)** Conversion Efficiency and **(b)** fill factor (FF) by varying thickness
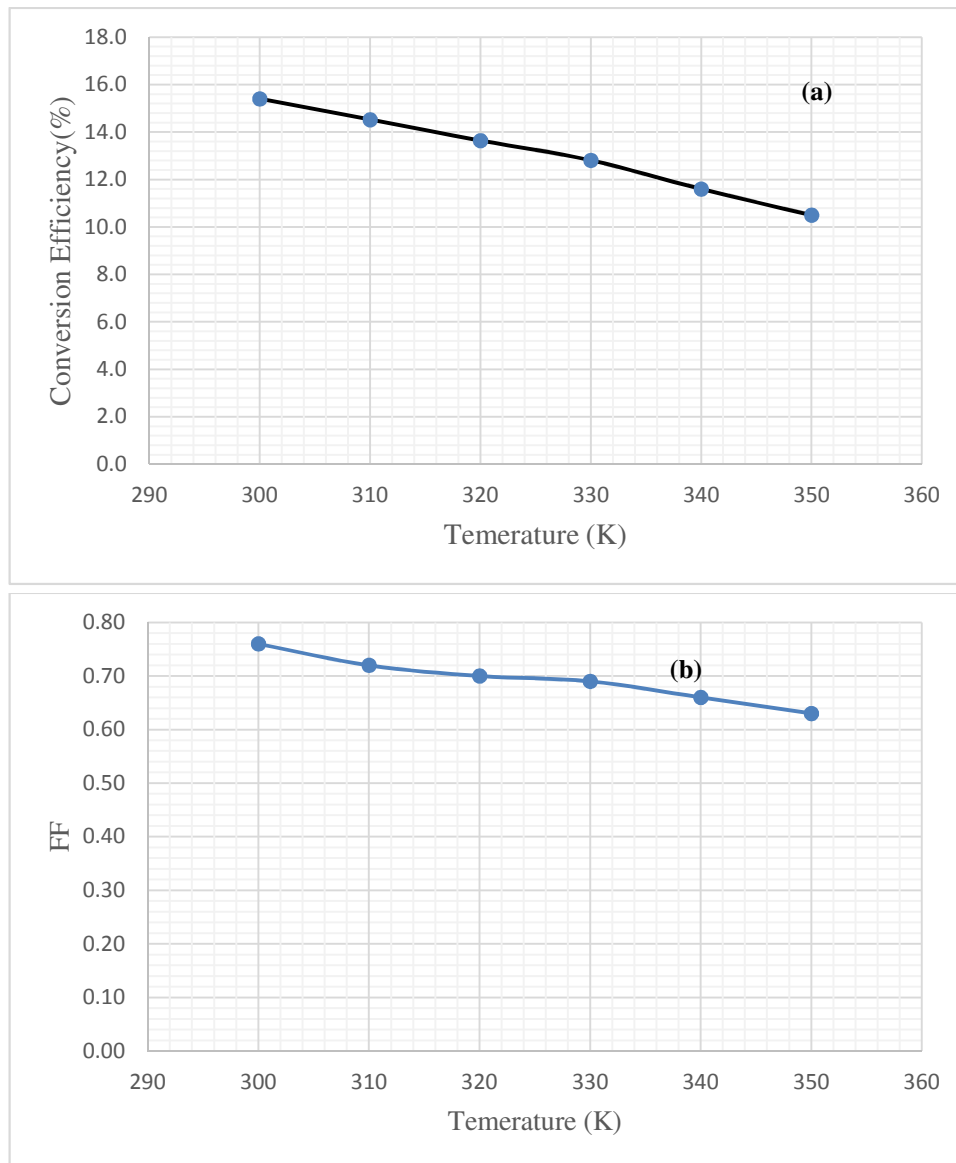
Fig. 5. Graph representing the variation of **(a)** Conversion Efficiency and **(b)** fill factor (FF) by varying the temperature.

5. Discussion

Fig. 4(a) it shows that as the thickness is changing from 1×10^{-7} m to 3×10^{-7} m, the efficiency slowly increases to about 14.7 % and later slowly decreases to 10.9 % at 6×10^{-7} m. The production of new charge carriers occurs due to increase in thickness which in turn increases the efficiency. But as the thickness increases further the efficiency slowly decreases due to increase in recombination rate of electron and hole pairs. The fill factor of model device decreases almost linearly as the thickness of active layer increases (Fig. 4(b)), which is in agreement with reports on bulk-heterojunction organic solar cells [13] and polymer bulk-heterojunction solar cells [14]. The electric field at the maximum power point on IV curve is smaller than that at short-circuit condition, bringing about lower dissociation rate and a higher recombination rate [15]. In thicker devices the

149

electric field is smaller due to the larger distance between the electrodes. Therefore recombination of charge carriers at the maximum power point is more prominent in thicker device, resulting in a low FF [14]. From Figs 5 (a) and (b), it can be deduced that as the temperature increases, there is a decrease in the performance of a device. The FF decrement as temperature increases is evident from Equations (1) and (2). As the temperature increases there is increase in the series resistance which leads to the decrease in the carrier diffusion length. The recombination rate also increases due to increase in temperature. Due to these the efficiency and fill factor drops.

6. Conclusion

In this work it was observed that as the thickness of the active layer (in this case $CH_3NH_3PbI_3$) increases, the efficiency of device increases up to when the thickness reaches 3×10^{-7} m. When the thickness exceeds 3×10^{-7} m, then the efficiency drops. At the optimal thickness of 3×10^{-7} m the devices were found to have power conversion efficiency up to 14.7%. On other hand the FF decreases as the thickness increases. The FF is highest at active layer thickness of 1×10^{-7} m. The effect of device temperature also studied and the optimal working temperature was found to be 300 K, where power conversion efficiency and FF are 15.4 % and 0.76 respectively. The optimal temperature obtained in this work for $CH_3NH_3PbI_3$ based Perovskite solar cell is same as the one found for $CH_3NH_3PbI_{3-x} Cl_x$ Perovskite solar cell [16].

References

[1]   Yuan, Y., Xu Run , Xu Hai-Tao, Hong Feng, Xu Fei and Wang Lin-Jun , Nature of the band gap of halide perovskites ABX_3(A= CH_3NH_3,Cs; B = Sn, Pb; X= Cl, Br, I): First-principles calculations. *Chin. Phys. B*. **24**(11): 5 (2015)

[2]   T. Baikie, Y. Fang, J. M. Kadro, M. Schreyer, F. Wei, S. G. Mhaisalkar, M. Graetzel and T. J. White, Synthesis and crystal chemistry of the hybrid perovskite (CH_3NH_3) PbI_3 for solid-state sensitised solar cell applications. *Journal of Materials Chemistry A,* **1**(18): 5628-5641 (2013)

[3]   Akihiro Kojima, Kenjiro Teshima, Yasuo Shirai and Tsutomu Miyasaka, Organometal halide perovskites as visible-light sensitizers for photovoltaic cells. *Journal of the American Chemical Society,* **131**(17): 6050-6051. (2009)

[4]   Völker S. F., S. Collavini, and J.L. Delgado, Organic charge carriers for perovskite solar cells. *Chem Sus Chem,* **8**(18): 3012-3028. (2015)

[5]   Wei E. I. Sha, Xingang Ren, Luzhou Chen and Wallace C. H. Choy, The efficiency limit of $CH_3NH_3PbI_3$ perovskite solar cells. *Applied Physics Letters,* **106**(22): 221104 (2015)

[6]   Takeo Oku, Taisuke Matsumoto, Atsushi Suzuki and Kohei Suzuki, Fabrication and characterization of a perovskite-type solar cell with a substrate size of 70 mm. *Coatings,* **5**(4): 646-655 (2015)

[7]   Oku T., Crystal structures of $CH_3NH_3PbI_3$ and related perovskite compounds used for solar cells, *Solar Cells-New Approaches and Reviews*., InTech. (2015)

[8] Liu D., M. K. Gangishetty, and T. L. Kelly, Effect of $CH_3 NH_3 PbI_3$ thickness on device efficiency in planar heterojunction perovskite solar cells. *Journal of Materials Chemistry A,* **2**(46): 19873-19881 (2014)

[9] Green M. A., Solar cell fill factors: General graph and empirical expressions. *Solid-State Electronics,* **24**(8): 788-789 (1981)

[10] Bimenyimana S., G. N. O. Asemota, and L. Lingling, Output Power Prediction of Photovoltaic Module Using Nonlinear Autoregressive Neural Network. *power,* **31**: p. 12 (2014)

[11] Roderick C. I. MacKenzie, *Gpvdm manual* (2016)

[12] Roderick C. I. MacKenzie, Thomas Kirchartz, George F. A. Dibb, and Jenny Nelson, Modeling nongeminate recombination in P3HT: PCBM solar cells. *The Journal of Physical Chemistry C,* **115**(19): 9806-9813 (2011)

[13] Nam Y. M., J. Huh and W. H. Jo, Optimization of thickness and morphology of active layer for high performance of bulk-heterojunction organic solar cells. *Solar Energy Materials and Solar Cells,* **94**(6): 1118-1124 (2010)

[14] Sievers D. W., V. Shrotriya and Y. Yang, Modeling optical effects and thickness dependent current in polymer bulk-heterojunction solar cells. *Journal of applied physics,* 2006. **100**(11): 114509 (2010)

[15] Koster L. J., E. C. P. Smits, V. D. Mihailetchi and P. W. M. Blom, Device model for the operation of polymer/fullerene bulk heterojunction solar cells. *Physical Review B,* **72**(8): 085205 (2005)

[16] Mandadapu U., S. V. Vedanayakam and K. Thyagarajan, Numerical Simulation of Ch3Nh3PbI3-XClx Perovskite solar cell using SCAPS-1D. *International Conference on Advances in Functional Materials (ICAFM-2017)* (2017)